Global Biogeochemical Cycles

RESEARCH ARTICLE
10.1029/2023GB007746

The Role of Coastal Yedoma Deposits and Continental Shelf Sediments in the Arctic Ocean Silicon Cycle

Nicholas E. Ray[1,2,3], Jannik Martens[1,4,5], Marco Ajmar[1], Tommaso Tesi[6], Evgeniy Yakushev[7,8], Ivan Gangnus[7], Jens Strauss[9], Lutz Schirrmeister[9], Igor Semiletov[10,11,12], and Birgit Wild[1,4]

[1]Department of Environmental Science, Stockholm University, Stockholm, Sweden, [2]Department of Ecology & Evolutionary Biology, Cornell University, Ithaca, NY, USA, [3]Now at School of Marine Science and Policy, University of Delaware, Lewes, DE, USA, [4]Bolin Centre for Climate Research, Stockholm University, Stockholm, Sweden, [5]Lamont-Doherty Earth Observatory of Columbia University, New York, NY, USA, [6]Institute of Polar Sciences, National Research Council, Bologna, Italy, [7]Shirshov Institute of Oceanology, Russian Academy of Sciences, Moscow, Russia, [8]Norwegian Institute for Water Research, Oslo, Norway, [9]Permafrost Research Section, Alfred Wegener Institute Helmholtz Centre for Polar and Marine Research, Potsdam, Germany, [10]Il'ichov Pacific Oceanological Institute (POI), Far-East Branch of the Russian Academy of Sciences, Vladivostok, Russia, [11]Tomsk State University, Tomsk, Russia, [12]Institute of Ecology, Higher School of Economics (HSE), Moscow, Russia

Key Points:

- Coastal erosion loads 30–90 Gmol Si yr^{-1} to the Arctic Ocean in the form of amorphous silicon
- Continental shelf sediments in the Arctic Ocean recycle more silicon than is loaded from rivers
- Approximately 4.5% of silicon loaded on the Arctic Ocean is buried in continental shelf sediments

Supporting Information:

Supporting Information may be found in the online version of this article.

Correspondence to:

N. E. Ray and B. Wild,
nickray@udel.edu;
Birgit.Wild@aces.su.se

Citation:

Ray, N. E., Martens, J., Ajmar, M., Tesi, T., Yakushev, E., Gangnus, I., et al. (2024). The role of coastal Yedoma deposits and continental shelf sediments in the Arctic Ocean silicon cycle. *Global Biogeochemical Cycles*, *38*, e2023GB007746. https://doi.org/10.1029/2023GB007746

Received 18 FEB 2023
Accepted 16 DEC 2023

Abstract The availability of silicon (Si) in the ocean plays an important role in regulating biogeochemical and ecological processes. The Si budget of the Arctic Ocean appears balanced, with inputs equivalent to outputs, though it is unclear how a changing climate might aggravate this balance. In this study, we focus on Si cycling in Arctic coastal areas and continental shelf sediments to better constrain the Arctic Ocean Si budget. We provide the first estimate of amorphous Si (ASi) loading from erosion of coastal Yedoma deposits (30–90 Gmol yr^{-1}), demonstrating comparable rates to particulate Si loading from rivers (10–90 Gmol yr^{-1}). We found a positive relationship between surface sediment ASi and organic matter content on continental shelves. Combining these values with published Arctic shelf sediment properties and burial rates we estimate 70 Gmol Si yr^{-1} is buried on Arctic continental shelves, equivalent to 4.5% of all Si inputs to the Arctic Ocean. Sediment dissolved Si fluxes increased with distance from river mouths along cruise transects of shelf regions influenced by major rivers in the Laptev and East Siberian seas. On an annual basis, we estimate that Arctic shelf sediments recycle approximately up to twice as much DSi (680 Gmol Si) as is loaded from rivers (340–500 Gmol Si).

1. Introduction

Silicon (Si) regulates phytoplankton community structure and the magnitude of the marine biological pump (Ragueneau et al., 2006; Tréguer et al., 2018), exerting a long-term control on climate (Tréguer & Pondaven, 2000). The availability of Si in different regions of the ocean is dictated by the balance of inputs, sinks, internal cycling, and transport between basins. The Si cycle in the modern ocean is considered to be at a steady state (Tréguer et al., 2021) and the Arctic Ocean is considered a net exporter of Si to other ocean basins, primarily to the highly productive North Atlantic (Torres-Valdés et al., 2013). Estimated Si inputs to the Arctic Ocean (1.56 ± 0.21 Tmol Si yr^{-1}; mean ± standard deviation) are balanced by estimated outputs (1.57 ± 0.35 Tmol Si yr^{-1}; Table 1). However, the Arctic Ocean is changing rapidly, particularly in the shallow shelf areas due to climate change with warmer waters, less ice, increased primary production, and accelerating coastal erosion (Gustafsson et al., 2011; Lewis et al., 2020; Meredith et al., 2019; Terhaar et al., 2020; Wild et al., 2019). Further, riverine inputs of Si to the Arctic Ocean may also be changing (Jankowski et al., 2023; Tank et al., 2023). As continental shelf areas make up more than half of the area of the Arctic Ocean (~53% of the Arctic Ocean; Jakobsson, 2002), understanding the Si cycle in these regions is necessary to project how the Arctic Ocean Si budget might respond to changing ocean and climate conditions.

Si is loaded on the Arctic Ocean both as dissolved Si (silicic acid, or DSi) and particulate amorphous Si (ASi) that includes biogenic Si (BSi) and non-mineral pedogenic Si. The main Si inputs to the Arctic Ocean are rivers (340–500 Gmol Si yr^{-1}) and ocean water inflow (1.08 ± 0.15 Tmol Si yr^{-1}; Table 1; Carey et al., 2020; Dürr et al., 2011; Holmes et al., 2012; Torres-Valdés et al., 2013). Ice sheet melt may load some Si to the Arctic Ocean (Hawkings et al., 2017; Meire et al., 2016), though the magnitude of this load is poorly quantified and the majority of Si derived from ice sheet melt is likely delivered to the North Atlantic. Most Si exported from the Arctic Ocean

Table 1
Silicon Budget for the Arctic Ocean

Inputs	(Gmol Si yr^{-1})	Source
Rivers	25–55 as BSi	Carey et al. (2020)
	90 as ASi	Hawkings et al. (2017)
	330 as DSi + 10 as PSi	Dürr et al. (2011)
	410 as DSi	Holmes et al. (2012)
	Total: 340–500[a]	
Ocean water inflow	660 ± 80 (Bering Strait)[b]	Torres-Valdés et al. (2013)
	420 ± 70 (Barents Sea Opening)[b]	
	Total: 1,080 ± 150	
Coastal Yedoma deposit erosion	*30—90 as ASi*	*This study*
Sum Inputs	**1,560 ± 210**	
Outputs		
Ocean water outflow	1,350 ± 160 (Davis Strait)[b]	(Torres-Valdés et al. (2013)
	220 ± 190 (Fram Strait)[b]	
Sediment accumulation (shelves)	*130 ± 70 (Kara Sea)* *70 ± 30 (Laptev Sea)* *130 ± 40 (East Siberian Sea)* *640 ± 240 (All Shelves)*	*This study*
Sediment burial (total)	<200[c]	Codispoti and Lowman (1973)
	Negligible	Anderson et al. (1983), Gordeev et al. (1996), Jones and Coote (1980)
Sediment burial (shelves)	*14 ± 8 (Kara Sea)*	*This study*
	8 ± 3 (Laptev Sea)	
	14 ± 4 (East Siberian Sea)	
	70 ± 30 (All Shelves)	
Sum Outputs	**1,570 ± 350 (no sediment burial)**	
	1,640 ± 380 (w. sediment burial)	
Internal Cycling		
Biogenic Si production	1,420	Tréguer et al. (2021)
Sediment regeneration (shelves)[d]	370	März et al. (2015)
	80 ± 130 (Kara Sea)	*This study*
	50 ± 50 (Laptev Sea)	
	210 ± 60 (East Siberian Sea)	
	680 ± 510 (All Shelves)	
Sediment regeneration (deep basin)	10–70	März et al. (2015)
	100–520[e]	Ng et al. (2020)
BSi sinking rate (particles >10 μm)	0.31–1.46 m d^{-1}	Heiskanen and Keck (1996)

Note. All units are in Gmol Si yr^{-1} unless otherwise indicated (ASi, amorphous Si; BSi, biogenic Si; DSi, dissolved Si; PSi, particulate Si). Values in italics are from this study. When mean rates are reported the value following ± is the standard deviation. As both ranges and standard deviations are reported, to estimate the range of inputs or outputs we assumed that the mean value fell in the middle of the range, and the standard deviation associated with that value was ¼ of the difference between the maximum and minimum values. Bold rows/values are the sum of inputs and outputs respectively.

[a]Total river load range estimated as lowest and highest DSi estimate (330 and 410) plus the lowest and highest ASi/BSi/PSi value (10 and 90 respectively). Mean ± SD (420 ± 40) estimated as described in the figure caption. [b]Torres-Valdés et al. (2013) report fluxes as kmol Si s^{-1}, which we have converted to Gmol Si yr^{-1}. [c]Codispoti and Lowman estimate a sink of $<2 \times 10^{14}$ mg-atoms yr^{-1} which we have converted to Gmol Si yr^{-1}. [d]The mean and SD associated with sediment regeneration is the shelf specific DSi flux multiplied by area and time. [e]Ng et al. reported sediment regeneration of 60–320 μmol DSi m^{-2} d^{-1} which we have converted to a whole basin estimate by multiplying by a Central Arctic Ocean Basin area of $4,489 \times 10^3$ km^2 (Jakobsson, 2002).

Table 2
Characteristics of Rivers Whose Influence on Arctic Ocean Continental Shelf Biogeochemistry Were Sampled in This Study

	Watershed permafrost cover (%)	Discharge (km^3 yr^{-1})	Dissolved silicon load (Gmol yr^{-1})	Particulate organic carbon load (Gg yr^{-1})	Dissolved organic carbon load (Tg yr^{-1})
Ob	5–13	427	50	600	4.1
Yenisey	37–55	636	60	300	4.2
Lena	94	588	50	80	5.7
Indigirka	100	50.6	6	–	–

Note. Data from Gordeev et al. (1996), Anderson et al. (2011), Gustafsson et al. (2011), Holmes et al. (2012), McClelland et al. (2016), and Wang et al. (2021).

passes through the Davis Strait and Fram Strait (1.35 ± 0.16 Tmol Si yr^{-1} and 220 ± 190 Gmol Si yr^{-1} respectively; Torres-Valdés et al., 2013). Early attempts to estimate the sediment Si sink in the Arctic Ocean considered the difference between river Si load and export of Si to other basins, and the magnitude of the sink was deemed negligible (Anderson et al., 1983; Codispoti & Lowman, 1973; Gordeev et al., 1996; Jones & Coote, 1980). On the other hand, past reports of surface sediment ASi content in the continental shelf region of the Arctic Ocean are high (up to 6%; Hoffmann et al., 2013; März et al., 2015; Nürnberg, 1996) compared to other continental shelf areas influenced by large rivers such as the Amazon Shelf (mean ASi of 0.25%; DeMaster et al., 1983) and the Louisiana-Texas Continental shelf (sediment ASi of 0.15%–1.3%; Turner & Rabalais, 1994), hinting at the potential for a possibly significant sediment Si sink. This discrepancy may be associated with the loading of substantial quantities of organic material from erosion along the Arctic Ocean coastline (Lantuit et al., 2012), particularly in Eastern Siberia, where the coastline is dominated by late Pleistocene Yedoma deposits that are prone to collapse due to their high ground ice content. These Yedoma deposits are interrupted by Holocene thermokarst depressions (alases) and thermo-erosional valleys (Schirrmeister, Kunitsky, et al., 2011). Erosion and permafrost thaw also takes place at Yedoma at riverbanks (Fuchs et al., 2020; Kanevskiy et al., 2016) as well as further inland, where the Yedoma domain and permafrost in general have been shown to be an important Si stock (Monhonval et al., 2021; Stimmler et al., 2023). Coastal erosion likely contributes additional Si to the Arctic Ocean (Pogojeva et al., 2018), but this flux has yet to be quantified.

Particulate organic matter containing Si from coastal erosion and river discharge is either buried or decomposed, recycling DSi to the water column. Indeed, the regeneration of nutrients such as Si from shelf sediments plays an important role in regional nutrient cycling (März et al., 2015; Nishino et al., 2009) and sediment nutrient regeneration may contribute 10%–20% of the nutrients required to sustain primary production in the Laptev and East Siberian seas (Sun et al., 2021). The rate of regeneration of Si from shelf sediments could also play an important role in regulating Si export from the Arctic basin due to the large area represented by shelf seas. On the continental shelf near the Mackenzie River delta, Link et al. (2013) reported sediment DSi fluxes of 314.5–3,494.7 μmol m^{-2} d^{-1}. On the outer shelf in the Laptev Sea and East Siberian Sea, Sun et al. (2021) reported annual sediment regeneration rates of 14.7 and 37.0 mmol DSi m^{-2} yr^{-1} (or 40.27 and 101.37 μmol DSi m^{-2} d^{-1} respectively) and suggested that DSi fluxes are likely to be higher nearer to shore and river mouths—a pattern possibly associated with erosion of coastal Yedoma deposits and Si containing particulates delivered from rivers draining permafrost regions. The balance of Si burial and regeneration on continental shelves in the Arctic Ocean may be an important lever regulating Si export from the region as the Kara, Laptev, and East Siberian shelves represent about 40% of the Arctic Ocean continental shelf area and are the recipient of large quantities of Si containing organic material from rivers such as Ob, Yenisey, Lena, and Kolyma in addition to coastal erosion.

In this study, we aimed to address these uncertainties and assessed Si source/sink dynamics on the Arctic continental shelves, focusing on the Kara, Laptev, and East Siberian Seas. We quantified the ASi content of near-coastal Yedoma deposits and provided the first estimate of ASi input to the Arctic Ocean from coastal erosion. Using data from a research cruise, we then determine how sediment Si recycling and accumulation on continental shelves in the Arctic Ocean might be related to distance from river mouths. Combining data generated in this study with previously published data sets, we calculate an annual sediment Si budget for continental shelves in the Kara, Laptev, and East Siberian seas and discuss these estimates in the context of an Arctic Ocean rapidly adjusting to climate change.

2. Methods

2.1. Study Area

The Kara, Laptev, and East Siberian seas extend over 2.4 Million km^2 (~40% of Arctic Ocean continental shelves) and are strongly influenced by large rivers draining permafrost-affected terrain (Table 2). The high river input to the Kara, Laptev and East Siberian seas is discernible not only in a high contribution of terrigenous organic

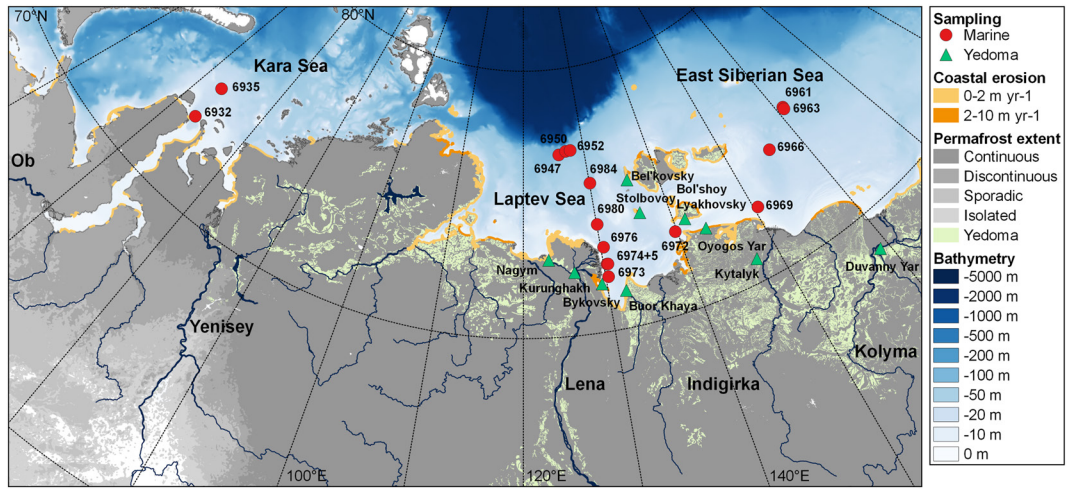

Figure 1. Location of sampling sites for multi-corer samples and Yedoma deposit sequences. Coastal erosion rates are from Lantuit et al. (2012), permafrost extent is from Obu et al. (2019), the Yedoma domain from Strauss et al. (2021) and bathymetry from International Bathymetric Chart of the Arctic Ocean (IBCAO) v4 (Jakobsson et al., 2020).

carbon to near-shore sediments and the water column (Karlsson et al., 2016; Martens et al., 2022) but also in a freshwater lens (Holmes et al., 2012). Like organic matter, the majority of Si appears to be loaded in the dissolved form (i.e., as DSi) rather than in the particulate form (i.e., as ASi; Carey et al., 2020; Heiskanen & Keck, 1996). The water column in the Lena and Indigirka river outflow regions typically displays strong stratification with a freshwater surface though between 10% and 30% of the time during ice-free periods this stratification is broken due to strong wind-driven upwelling (Osadchiev et al., 2020). Upwelling has been shown to be important in cycling nutrients to surface waters in other shallow coastal regions of the Arctic (e.g., Tremblay et al., 2014).

The Laptev and East Siberian seas are additionally influenced by coastal erosion that can locally exceed 5 m per year (Lantuit et al., 2012). Coastal erosion in this area is driven by the high frequency of Yedoma deposits along the coasts, that is, late-Pleistocene permafrost deposits that are vulnerable to collapse due to their high ice content. Coastal erosion of Yedoma deposits is highest near the Buor Kaya Bay (Günther et al., 2013; Schirrmeister et al., 2017; Strauss et al., 2015), the Dmitri Laptev Strait, and the New Siberian Islands (Schirrmeister, Kunitsky, et al., 2011) and leads to significant loading of organic matter nearshore in the Laptev and East Siberian sea (Bröder et al., 2016; Matsubara et al., 2022).

2.2. Marine and Terrestrial Sampling Sites

Samples of near-coastal Yedoma sequences, including overlying Holocene deposits and modern active layer soils, were collected from exposed sections of coastal or river Yedoma during various joint German-Russian expeditions. The 56 samples included in this study are from 10 locations visited between 1998 and 2011; details of the sites are described in previous publications (Schirrmeister, Grosse, et al., 2011; Strauss et al., 2012) and a complete sample list is provided in Table S1 in Supporting Information S1.

Water and sediment samples were collected during the International Siberian Shelf Study 2020 expedition (ISSS-2020) aboard the Russian vessel *RV Akademik Mstislav Keldysh* between late September and early November 2020. For this study, we used water column profiles from 31 stations and sediment cores from 16 stations along transects of river water influence in the Kara, Laptev, and East Siberian seas (Figure 1, Table S2 in Supporting Information S1). In the Kara Sea, cores were collected at two stations in the Ob River plume, one near shore (station AMK82-6932, further abbreviated by station numbers only) and one further from shore (6935). In the Laptev Sea, we collected cores at 10 stations, aiming to capture the influence of the Lena River. Stations 6973, 6974, 6975, 6976, 6980, 6984, 6947, 6950, and 6952 were located north of the Lena Delta and Station 6972 in the Dmitry-Laptev Strait to the east. Though the Dmitry-Laptev Strait is technically in the East Siberian Sea, here we consider it in the context of the Laptev Sea, with Lena River and Siberian coastal current influence. In the East Siberian Sea, stations 6961, 6963, 6966, and 6969 capture the Indigirka River plume at varying distances from

shore. Station 6969, located near the shore, is also influenced by freshwater flowing through the Dmitry-Laptev Strait.

2.3. Water Column Sampling and Measurements

The water column profile was measured at discrete depths (surface, near-bottom, pycnocline, and haphazardly selected depths between; each depth sampled at each station is available in the published data set) upon arrival to each station using a Seabird SBE911 plus conductivity-temperature-depth (CTD) equipped with Niskin bottles and Seapoint chlorophyll fluorometer to determine temperature, salinity, and chlorophyll-a concentration. In total, the water column profile in areas of river influence was measured at 5 stations in the Kara Sea, 17 stations in the Laptev Sea, and 9 stations in the East Siberian Sea. Water samples from the Niskin bottles were transferred to acid-washed polyethylene containers and analyzed immediately using colorimetric methods (QuAAtro Analyzer equipped with an autosampler; Seal Analytical, Mequon, USA) to quantify DSi concentration following method Q-066-05 (ammonium molybdate method; Hydes et al., 2010; Strickland and Parsons, 1968). Generally, water samples were filtered using 0.7 μm GF/F grade glass microfiber filters prior to analysis, except in several cases when turbidity was low (4 out of 31 stations; all unfiltered samples were collected from the outer Laptev Sea—stations 6947, 6948, 6950, 6952). We note that it is preferable to use other filter types (e.g., nitrocellulose or polycarbonate) for DSi sampling as it is possible that GF/F filters may introduce small amounts of error to the measurement. However, during the cruise analyses of dissolved nutrient concentrations (including dissolved nitrogen and phosphorus) were made from a single sample, which was often filtered through a GF/F filter. For this reason, we do not focus on specific DSi concentrations when discussing water column DSi, but instead on broader concentration gradients. The minimum detection limit for DSi was 0.40 μmol DSi L^{-1} while at sea and 0.23 μmol DSi L^{-1} on land (for analysis of digested sediment and coastal Yedoma sequence samples).

2.4. Sediment Collection and Flux Incubations

Following the CTD deployment, we collected sediment cores (polycarbonate 9.6 cm inner diameter, 60 cm length) using a multi-corer and moved the cores to a water bath to maintain constant temperature throughout the incubation. We used a batch incubation approach to measure DSi and O_2 fluxes between the sediment and overlying water, being careful to only use cores that had at least 8 cm of sediment (average sediment depth 15 cm) and an intact sediment structure. The water overlying the sediment in each core was left in place, and in cases where there was not enough overlying water to completely fill the core, we siphoned additional water from other sediment cores collected at the same site that were used for other analyses. Since we used unfiltered water for incubations, we also siphoned water from other cores to use as control cores (i.e., an incubation of water only) to account for DSi and O_2 fluxes occurring in water overlying sediments. Surface sediments (0–1 cm) from adjacent cores in the same multi-corer cast were collected and oven-dried at 60°C onboard and stored until analysis of sediment chemical properties (total organic carbon (TOC), stable carbon isotope ratio ($\delta^{13}C$), and ASi content).

Prior to beginning each incubation, we measured the depth of sediment from the top of the core to estimate the volume of overlying water (average volume 3.21 L). Next, we attached polycarbonate lids equipped with optical sensors for measuring O_2 concentration (Precision Sensing GmbH, Regensburg, Germany), and a magnetic stir bar at least 25 cm above the sediment, set to rotate at approximately 40 rpm to maintain water mixing without creating advective flow (Glud et al., 2007). Immediately after closing the cores, we collected samples of overlying water in the sediment core and water control core into acid-washed high density polyethylene (HDPE) flasks. The collected water was not filtered and analyzed immediately for DSi concentration using the same methods described earlier for water column sampling. Sediment incubations were also used to measure fluxes of dissolved gases (Wild et al., 2023), which yielded a total volume replacement of <10%. The volume of sample replaced during this time was replaced with water siphoned from adjacent cores and kept in a carboy. We checked the O_2 concentration in each core several times throughout the course of the incubation with the aim of at least a 2.0 mg L^{-1} drop in O_2 concentration without the core becoming hypoxic (<2.0 mg O_2 L^{-1}). This was balanced by ensuring that all incubations were complete before the cruise ended, and on average, incubations lasted 12.6 days. Following the fifth recorded O_2 concentration measurement, we collected a second water sample for the analysis of DSi concentration. The average incubation temperature was 3.3 ± 1.5°C.

O_2 fluxes were calculated using a regression of concentration over time, and were considered significant when the regression $R^2 \geq 0.65$ and $p \leq 0.10$ (Prairie, 1996; Wild et al., 2023). All O_2 fluxes met these standards except for

two incubations, which had positive O_2 fluxes, indicating an improper seal of the lid (Station 6961 and 6963 in the outer East Siberian Sea). We excluded these two O_2 fluxes from our analyses, but DSi fluxes in those cores were likely unaffected, so we retained these data points. DSi fluxes were calculated as the difference in concentration between the initial and final sample over time. We then converted these rates to μmol O_2 m^{-2} d^{-1} or μmol DSi m^{-2} d^{-1} considering the volume of water in the core, and the core cross-sectional area. To correct for processes occurring in the water column and due to volume replacement, we subtracted the fluxes of DSi and O_2 in each water control core from the associated sediment core. The DSi flux in cores containing sediment was greater in magnitude than water control cores in all but one case (station 6976), and control cores displayed a range of DSi uptake and release (mean DSi flux = −0.13 μmol DSi L^{-1} d^{-1}).

2.5. Sediment and Soil Properties

Surface sediments were analyzed for TOC and $\delta^{13}C$ by weighing sample aliquots in silver capsules and acidifying with HCl to remove carbonates. Samples were then analyzed using a Finnigan Delta Plus XP mass spectrometer coupled to a Thermo Fisher Scientific Flash 2000 Isotope Ratio Mass Spectrometer Element Analyzer via a Conflo II interface. For Yedoma sequences, data on TOC were available from previous publications (see Table S1 in Supporting Information S1).

Both marine and terrestrial sediment samples were analyzed for ASi content (% mass) using a wet alkaline extraction method (Conley, 1998; Conley & Schelske, 2001; DeMaster, 1981). Briefly, 30 mg of oven dried and ground material was leached with 40 ml 1% sodium carbonate in acid-washed HDPE containers placed in an 85°C water bath equipped with a shaker table. After 3, 4, and 5 hr, a 1 ml aliquot of the leachate was pipetted into 9 ml of 0.021 N hydrochloric acid. These samples were analyzed using the same method described previously for water column and sediment flux DSi measurements. We then calculated ASi concentrations using the DSi concentrations (Conley, 1998). In order to ensure we did not overestimate ASi concentrations due to low ASi content and to account for the dissolution of clays, we used a slope correction approach (Conley, 1998). When least squares regression indicated a significant increase ($p < 0.05$, $R^2 \geq 0.65$) in ASi concentration over the three time points ($n = 12$ shelf sediment samples and $n = 67$ for terrestrial samples), we considered the intercept of the least squares regression as the ASi concentration. In cases when $p \geq 0.05$ and $R^2 < 0.65$ ($n = 4$ shelf sediment samples and $n = 5$ for terrestrial samples) we considered ASi concentration as the mean of the three time points when leachate was collected for analysis (Conley, 1998; DeMaster, 1981). All ASi values are reported as % SiO_2 by mass. Throughout ASi analysis, we included external reference material that had previously been included in an interlaboratory comparison to ensure accuracy and comparability across studies (Conley, 1998). Our estimate of the BSi content of the references was similar to mean values of both the low standard (our analysis: 2.41 ± 0.07% BSi; interlaboratory comparison: 2.82 ± 1.17% BSi) and the high standard (our analysis: 6.83 ± 0.39% BSi; interlaboratory comparison: 6.49 ± 2.09% BSi).

2.6. Statistical Analysis

All data analysis was conducted using R Statistical Software (R Core Team, 2014). We tested whether sediment DSi flux could be predicted by surface sediment properties (%TOC, $\delta^{13}C$, and %ASi) and for relationships between sediment properties using linear regressions. We used linear models to test the relationship between sediment properties and fluxes as a function of distance from the river mouth in each sea. In these models, we considered the station in the Dmitry Laptev Strait (6972) to be in the Laptev Sea, as it is most influenced by the Lena River. Student's *t*-test was applied to test for differences between Yedoma deposits and overlying Holocene deposits and modern active layer samples. We considered the results of statistical tests to be statistically significant when $p < 0.05$.

2.7. Scaling Approach and Budget Estimation

We combined the data generated in this study with previously published data to estimate the annual load of Si to the Arctic Ocean from coastal erosion, burial of Si in shelf sediments, and sediment Si regeneration. The ASi input by coastal erosion to the Arctic Ocean was calculated by combining the ASi:TOC ratios of Yedoma sequences with previous estimates of the coastal erosion TOC flux. The input of TOC to the Arctic Ocean by coastal erosion has been estimated by Wegner et al. (2015) as 4.9–14.0 Tg TOC yr^{-1}. This flux is dominated

by the collapse of Yedoma deposits along the coasts of the Laptev and East Siberian seas that alone contribute 2.9–11.0 Tg TOC yr^{-1} (Wegner et al., 2015). We consequently consider the average ASi:TOC ratio determined for the 56 samples of East Siberian Yedoma sequences analyzed here, including overlying Holocene active layer material, as a representative of the material released by coastal erosion to the Arctic Ocean. We report total Si loaded from erosion assuming all soils eroded have similar ASi:TOC and report the contribution of Yedoma sequences and overlying Holocene deposits and modern active layer material to this total.

Linear relationships between sediment ASi and TOC relationships have been used previously to estimate whole shelf Si accumulation and burial (e.g., DeMaster, 2002; DeMaster et al., 1996). Thus, the relationship observed in this study between surface sediment ASi and TOC allowed us to take advantage of the Circum-Arctic Sediment CArbon DatabasE (CASCADE; Martens et al., 2021) to estimate the concentration of surface sediment ASi across the Arctic shelf seas. An extensive data set of sediment mass accumulation rates (MAR) from around the circum-Arctic based on a depth-integrated inventory of excess ^{210}Pb (Martens et al., 2022) was used to estimate the annual accumulation of ASi in sediments of the Kara, Laptev, and East Siberian seas. For estimating the elemental MAR of ASi in Kara, Laptev and East Siberian sea sediments, the linear model between ASi (% mass) and organic carbon (% mass) was applied to the published TOC concentration and MAR data sets of the different circum-Arctic shelf seas using ArcGIS 10.8. ASi concentrations estimated using this approach agreed well with the measured values of our 16 study locations ($R^2 = 0.306$; $p = 0.026$; $y = 0.45x + 0.27$) and landed in a very similar range (0.07%–0.65% ASi for measured and 0.23%–0.86% ASi for estimated values). Interpolated ASi concentrations were then multiplied with MAR based on depth-integrated inventories of excess ^{210}Pb in sediment profiles from the Kara, Laptev, and East Siberian seas.

We found no relationships between sediment properties and sediment DSi flux, and thus used a simpler approach to scale DSi fluxes across all Arctic Ocean continental shelves. Specifically, we used the mean measured rate of DSi regeneration on each shelf region and scaled these to the area of each shelf (Kara Sea: 926×10^3 km^2, Laptev Sea: 498×10^3 km^2, and East Siberian Sea: 985×10^3 km^2; Jakobsson, 2002), assuming rates of Si regeneration were constant throughout the year. Our estimate of DSi regeneration for the remaining shelf area uses the mean rate of DSi regeneration for all samples collected in this study and assumed this rate to be constant across the remaining shelf area of the Arctic Ocean ($2{,}641 \times 10^3$ km^2).

3. Results

3.1. Silicon Input to the Arctic Ocean by Coastal Erosion

The ASi content of analyzed Yedoma sequences, including overlying Holocene deposits and modern active layer material, averaged 0.64 ± 0.35% ASi (from here all values reported as mean ± SD) of the dry weight, with a range of 0.08%–1.71% ASi ($n = 56$; see Table S1 in Supporting Information S1 for all data). Concentrations were lower in the Yedoma deposit material (0.56 ± 0.27% ASi, $n = 34$) than in the Holocene deposits and active layer (0.80 ± 0.44%, $n = 19$), but this difference disappeared when concentrations were normalized by TOC (average ASi:TOC ratio 0.39 ± 0.33, $n = 56$; TOC data in Table S1 in Supporting Information S1).

We estimated the coastal erosion ASi input to the Arctic Ocean by combining ASi:TOC ratios of Yedoma and Holocene deposits and modern active layer samples with previous estimates of the coastal erosion TOC flux, yielding a coastal erosion Si load estimate of 1.9–5.5 Tg ASi yr^{-1} or 30–90 Gmol Si yr^{-1}, with 20–70 Gmol Si derived from coastal Yedoma sequences and the overlying Holocene deposits and modern active layer.

3.2. Oceanographic Context and Water Column Dissolved Silicon

We measured a clear signal of riverine influence along the sampling transects in each sea, indicated by relatively warm and low salinity surface waters overlying colder and saltier deep water (Figure 2). DSi concentrations were typically highest in surface waters in both the Kara and Laptev seas, likely reflecting the influence of the Ob and Lena rivers respectively. The influence of the Lena River was also apparent in the Dmitry Laptev Strait, where surface salinity, temperature, and DSi concentration matched those recorded at the Lena River mouth, though this site was also likely influenced by Yana River water. DSi concentrations were similar in surface and deep water at deeper stations in the Laptev Sea (6947, 6950, 6052, 6984), to lowest concentrations at 25 m depth (Figure 2). Bottom water DSi concentrations in the East Siberian Sea were higher than surface water at all stations except

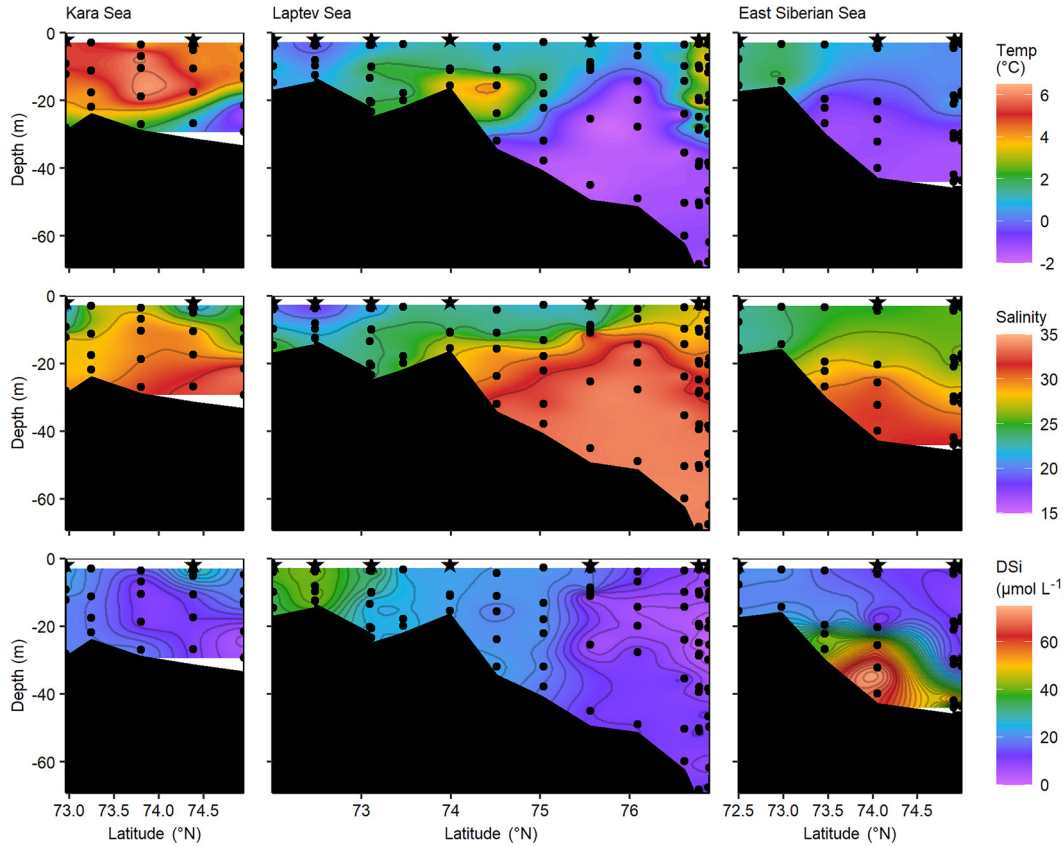

Figure 2. Depth profiles of temperature, salinity, and dissolved silicon concentrations along transects between sediment coring stations (marked with a star) in the Kara Sea (left column), Laptev Sea (middle column), and East Siberian Sea (right column). Each dot represents a measurement (5 profiles in the Kara Sea, 17 in the Laptev Sea, and 9 in the East Siberian Sea).

the station nearest shore (6969), which was shallow and well mixed, and concentrations were uniform throughout the water column.

3.3. Sediment Silicon Accumulation and Burial Estimates

The TOC content of shelf sediment samples was never higher than 2.3% (mean TOC 0.9 ± 0.56%). We measured both the highest and lowest TOC values in the Laptev Sea (Figure 3). There was no clear pattern between sediment TOC and distance from the river mouth ($p = 0.516$, marginal $R^2 = 0.029$). However, $\delta^{13}C$ tended to become less depleted as distance from river mouths increased in all three seas ($p = 0.003$, marginal $R^2 = 0.433$; Figure 3).

The mean ASi content of all surface sediments was 0.41 ± 0.20% ASi. Mean % ASi was similar between the Kara (0.59 ± 0.08% ASi) and East Siberian seas (0.54 ± 0.12% ASi), which were both slightly higher than the Laptev Sea, which was also the most variable (0.32 ± 0.20% ASi; Figure 3). Sediment ASi content was well predicted by % TOC ($p = 0.003$, $R^2 = 0.474$; Figure 4), and exhibited a positive relationship, though this pattern appears driven by the Kara and Laptev seas.

Combining our observations with previously published data sets, we estimate ASi accumulation of 130 ± 70 Gmol Si yr^{-1} for the Kara Sea, 70 ± 30 Gmol Si yr^{-1} for the Laptev Sea, and 130 ± 40 Gmol Si yr^{-1} for the East Siberian Sea (Figure 6; Table 1). If the relationship observed between ASi and TOC holds across all continental shelf areas in the Arctic Ocean, we estimate Arctic shelf-wide accumulation of 640 ± 240 Gmol Si yr^{-1}. Of course, accumulation and permanent burial are not the same. We can roughly estimate the burial efficiency by dividing the mean global rate of Si burial (9.2 Tmol Si yr^{-1}) by the mean rate of Si rain (84 Tmol Si yr^{-1}) to estimate a burial efficiency of ~11% (Tréguer et al., 2021). Applying this burial efficiency factor leads to a total Arctic shelf-wide burial of 70 ± 30 Gmol Si yr^{-1} (Table 1).

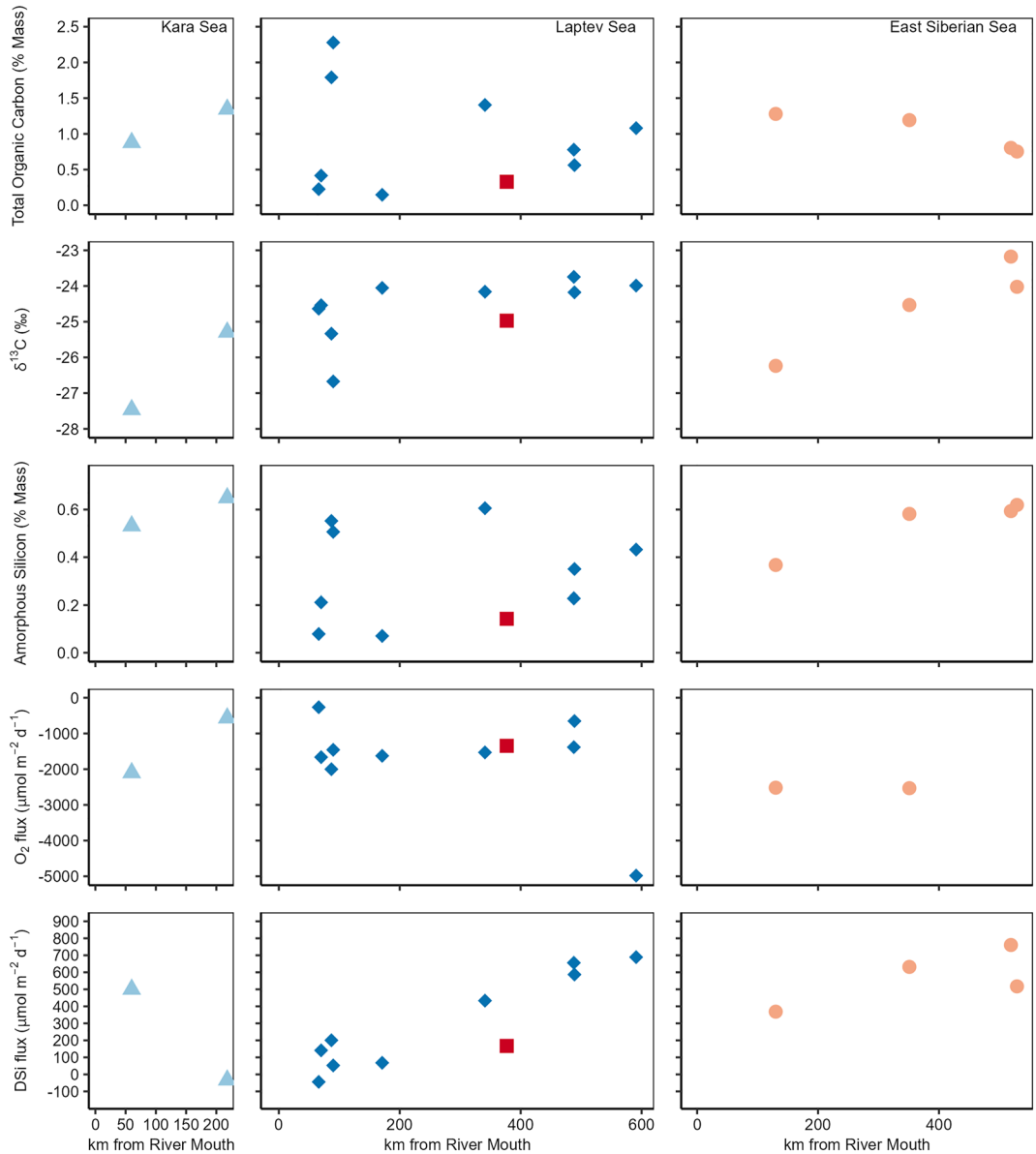

Figure 3. Sediment total organic carbon, $\delta^{13}C$ of organic carbon, amorphous silicon content, oxygen consumption, and dissolved silicon regeneration in the Kara (triangles), Laptev (diamonds), and East Siberian seas (circles) in relation to distance from the mouths of the Ob River, Lena River, and Indigirka River. We have included the Dmitry Laptev Strait (square) in the Laptev Sea panel as it is influenced by the Lena River. Two cores in the East Siberian Sea had positive fluxes for oxygen, indicating gas exchange with the atmosphere; therefore, these were excluded from analysis.

3.4. Sediment Silicon Regeneration

On average, sediments consumed 1,759.0 ± 1,146.5 μmol O_2 m^{-2} d^{-1}. Both the highest (−4,980.8 μmol O_2 m^{-2} d^{-1}; Station 6947) and lowest (−265.56 μmol O_2 m^{-2} d^{-1}; Station 6974) O_2 fluxes were measured in the Laptev Sea, but there were no systematic differences in sediment O_2 fluxes across the three seas. Neither sediment TOC ($p = 0.446$, $R^2 = 0.049$) nor $\delta^{13}C$ ($p = 0.950$, $R^2 = 0.000$) were useful for predicting O_2 flux.

Shelf sediments recycled DSi to the water column at a mean rate of 356.05 ± 275.69 μmol DSi m^{-2} d^{-1}. Si regeneration was highest in the East Siberian Sea (569.72 ± 166.78 μmol DSi m^{-2} d^{-1}) followed by the Laptev Sea (295.10 ± 271.72 μmol DSi m^{-2} d^{-1}, including the station in the Dmitry-Laptev Strait) and then the Kara Sea (233.47 ± 377.32 μmol DSi m^{-2} d^{-1}). We found no relationships between sediment DSi flux and %ASi ($p = 0.167$, $R^2 = 0.070$), % TOC ($p = 0.966$, $R^2 = 0.000$), or $\delta^{13}C$ ($p = 0.154$, $R^2 = 0.078$). However, sediment DSi

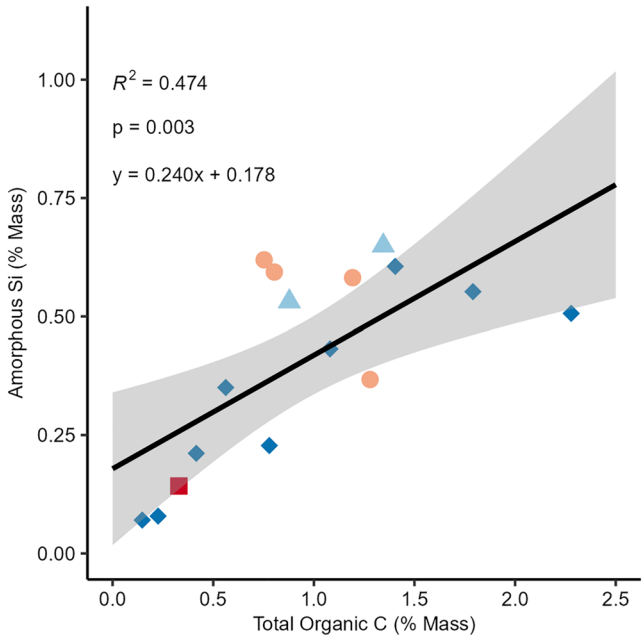

Figure 4. Relationship between sediment total organic carbon and amorphous silicon content from sediments collected in the Kara Sea (light blue triangles), Laptev Sea (dark blue diamonds), Dmitry Laptev Strait (red square), and East Siberian Sea (pink circles). The gray-shaded area indicates the 95% confidence intervals around the regression.

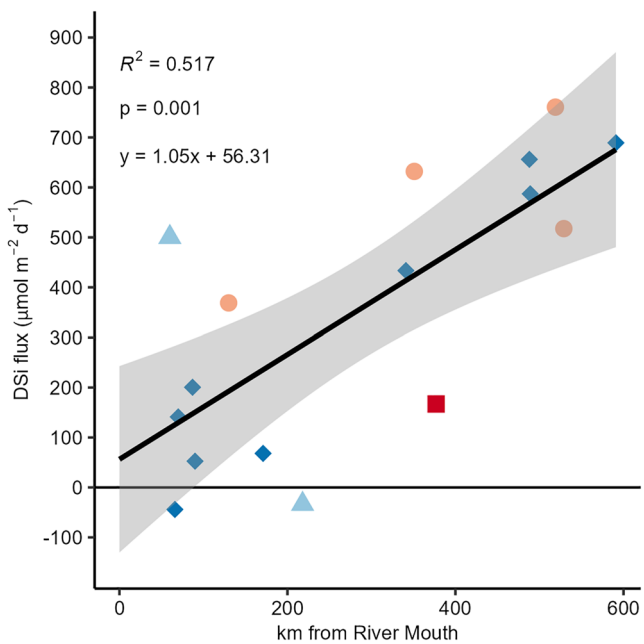

Figure 5. Relationship between sediment silicon regeneration and distance from the mouth of the Ob River (Kara Sea; light blue triangles), Lena River (Laptev Sea and Dmitry Laptev Strait; dark blue diamonds and red square respectively), and Indigirka River (East Siberian Sea; pink circles). The gray-shaded area indicates the 95% confidence interval around the regression.

flux increased with distance from the river mouth (p = 0.001, R^2 = 0.517; Figure 5), with highest rates of sediment DSi regeneration at stations furthest from the mouth of the Lena and Indigirka Rivers in the Laptev and East Siberian sea.

On an annual basis, we estimate that 340 Gmol Si yr^{-1} are regenerated from the Kara (80 ± 130 Gmol Si yr^{-1}), Laptev (50 ± 50 Gmol Si yr^{-1}), and East Siberian Seas (210 ± 60 Gmol Si yr^{-1}), which cover ~47.7% of the continental shelf area of the Arctic Ocean. We estimate annual DSi regeneration on other Arctic Continental shelves not sampled here to equal 340 ± 270 Gmol Si yr^{-1}. In total, we estimate that Arctic Ocean shelves regenerate 680 ± 510 Gmol Si yr^{-1}.

4. Discussion

4.1. Equivocal Importance of Coastal Erosion in the Arctic Ocean Si Budget

Our measurements of ASi content in coastal Yedoma deposits and the overlying Holocene deposits and modern active layer (0.08%–1.71%) are comparable to recent studies that report between <0.1% and 2.3% ASi in the top 1 m of permafrost soils (Alfredsson et al., 2015, 2016). Our measured ASi:TOC ratios (0.39 ± 0.33) were also similar, if not slightly higher than those derived from these earlier studies (0.08–0.38, excluding uplifted peatland sites that show very low ASi:TOC; Alfredsson et al., 2015, 2016). Together, these similarities suggest that there is little difference between coastal and inland permafrost regarding ASi content. Thus, in our scaling estimate, we considered all coastal erosion, not Yedoma alone.

Using the ASi:TOC ratio determined here, we estimated that coastal erosion delivers 30–90 Gmol Si yr^{-1} to the Arctic Ocean, with 20–70 Gmol Si derived from coastal Yedoma deposits. While this coastal erosion flux approximates 6%–26% of the Si loaded by rivers (340–500 Gmol Si yr^{-1}), it only increases total estimated Si inputs to the Arctic Ocean by 2%–6%. However, in near-shore regions of the Laptev and East Siberian seas that receive most of the coastal erosion-derived Si (20–70 Gmol Si yr^{-1}), a stronger biogeochemical impact of coastal erosion might be observed at a local scale.

For example, limiting nutrients for phytoplankton production may differ in areas where erosion and river outflow are of differing importance. There is support for the hypothesis that nitrogen (N) derived from coastal erosion is an important contributor to primary production in the Arctic Ocean (Terhaar et al., 2021), and coastal erosion may also regulate the N:Si ratio of shelf areas in the Arctic Ocean. Terhaar et al. (2021) estimated that 1.0–2.5 Tg N yr^{-1} (or 70–180 Gmol N yr^{-1}) enter the Arctic Ocean from coastal erosion. Compared with our estimated Si load from coastal erosion (30–90 Gmol Si yr^{-1}), we can estimate an N:Si molar ratio of ~2.1 for material loaded on the Arctic Ocean via coastal erosion. The molar ratio of N:Si from rivers is 0.22 (estimated from Holmes et al., 2012, p. 90 Gmol N yr^{-1} and 406 Gmol Si yr^{-1}). Taken together, the average M N:Si load of rivers and coastal erosion is likely around 0.5, demonstrating that coastal erosion is likely more important in regulating N availability and might lead to Si becoming a limiting nutrient for diatom growth in some regions where the majority of nutrients are delivered from coastal erosion.

4.2. Sediment Si Accumulation

Sediment $\delta^{13}C$ followed previously reported trends and became less depleted further from river mouths, indicative of a shift from terrestrial to marine

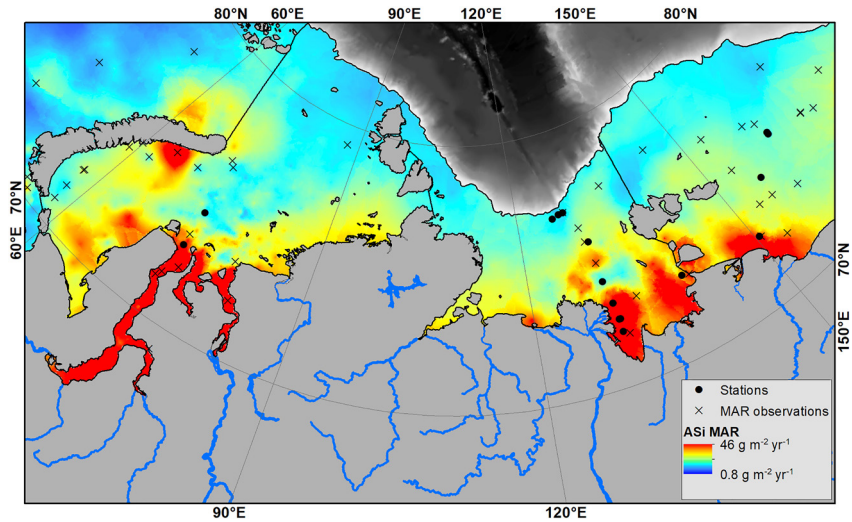

Figure 6. Accumulation of amorphous silicon (ASi) in surface sediments of the Kara, Laptev and East Siberian Seas. Black circles indicate stations analyzed for ASi concentrations during the ISSS-2020 expedition. Crosses indicate locations with published mass accumulation rates (MAR) based on $^{210}Pb_{xs}$ inventories of sediment cores (Martens et al., 2022). Interpolated values were estimated by applying the linear relationship between ASi and organic matter identified here (Figure 4) to the CASCADE database (Martens et al., 2021), which summarizes surface organic matter and to the MAR rates from Martens et al. (2022).

organic C sources (Bröder et al., 2018, 2019; Martens et al., 2021, 2022; Matsubara et al., 2022). However, we found no relationships between sediment ASi or TOC and distance from river mouths, possibly due to relatively low concentrations of both, indicative of rapid remineralization of organic material loaded on sediments in this region (Anderson et al., 2011). This lack of relationships apart from the positive relationship between % ASi and % TOC suggests that the source of organic material may be less important than the quantity loaded on sediments in regulating ASi accumulation on Arctic continental shelves. Alternatively, it is possible this finding may be associated with our relatively small sample size coupled with high spatial variability, as previous studies have demonstrated clear patterns of decreasing TOC with distance from the river mouth, albeit with many more observations (e.g., Bröder et al., 2019; Martens et al., 2022).

The observed relationship between sediment ASi and TOC was driven by samples from the Kara and Laptev seas—samples from the East Siberian Sea appear to have an opposite pattern, though a regression of ASi as a function of TOC for these four points is not significant ($p = 0.247$; Figure 4). A possible explanation for the apparent different behavior of sediment ASi:TOC in the East Siberian Sea relates to the influence of Pacific water. The outer two stations (6961 and 6963) that have high ASi content and low TOC content exhibit relatively high marine influence (considering $\delta^{13}C$). Sediments at these stations also exhibited relatively high DSi flux. These sediments might have been influenced by a recently deposited diatom bloom at the confluence of shelf and Pacific water, which may lead to relatively high ASi loading compared to terrestrially derived particulates.

Our measured ASi concentrations are lower than previously reported surface ASi concentrations between the Lena Delta and New Siberian Islands in the Laptev Sea (nearly 6% ASi) and the Kara Sea near our sampling stations (3%–5% ASi; Nürnberg, 1996). Our measurements are in the range of reported values for the western part of the Laptev Sea of 0%–2% ASi (Nürnberg, 1996) and are quite similar to recent measurements made in the Barents Sea (0.26%–0.52% ASi; Ward et al., 2022a). It is not clear whether the differences between our measurements and those of Nürnberg (1996) are driven by methodology, changing conditions in the Arctic Ocean, or some combination of these factors. Similar to us, Nürnberg (1996) employed a wet alkaline extraction method following DeMaster (1981), though an interlaboratory comparison study found that various iterations of this methodology might lead to large differences in the determination of BSi content, particularly from samples with relatively low BSi content (Conley, 1998). The observed difference might also reflect changing conditions in the Arctic Ocean, both regarding enhanced rates of water column primary production and decomposition of organic material in sediments. The Arctic Ocean has warmed ~1.5 °C when samples in this study were collected compared to when samples analyzed by Nürnberg (1996) were collected (1991–1994)). These warmer waters

might have led to more rapid dissolution of surface sediment ASi in recent years, as both bacterial decomposition of organic material and chemical dissolution of ASi increase with temperature (Kamatani, 1982; Van Cappellen & Qiu, 1997). It is possible that these two processes may have a synergistic effect. It is unlikely that the observed differences in surface ASi content and those reported by Nürnberg (1996) are due to spatial variability, as even though we observed highly variable sediment ASi content as a function of distance from the river outflow, all values were below 1%.

4.3. Sediment Silicon Recycling and Oxygen Consumption

Our measurements of sediment DSi regeneration are at least five times higher than those previously reported by Sun et al. (2021) for the outer East Siberian Shelf (101.4 μmol DSi m^{-2} d^{-1}) and Laptev seas (40.3 μmol DSi m^{-2} d^{-1}) made during the SWERUS-C3 expedition in 2014. While Sun et al. (2021) suggested sediment DSi regeneration might be highest near shore, we found the opposite of this prediction—rate of sediment DSi regeneration were highest at stations furthest from shore. The lack of relationships between sediment DSi flux and sediment properties (% TOC, %ASi, $\delta^{13}C$) make the identification of a mechanism that might drive this pattern challenging, and we make no suggestions in this regard.

Our measured rates of sediment O_2 consumption are of similar magnitude to those measured on the Mackenzie Shelf (500–11,500 μmol O_2 m^{-2} d^{-1}; Link et al., 2013), yet our measured DSi fluxes are an order of magnitude lower. Perhaps this discrepancy can be explained by the C content of the particulate load of the rivers—while the Mackenzie River has a similar TOC load as the Siberian rivers, only 64% of the organic C load of the Mackenzie is in dissolved form, unlike the Siberian rivers which typically export 87%–95% of their organic C in dissolved form (Holmes et al., 2012; McClelland et al., 2016). Further, the Mackenzie has a smaller annual discharge than the Lena and Ob rivers, possibly leading to relatively weaker stratification and more rapid loading of particulates to shelf sediments before Si dissolution in the water column can occur, yielding higher rates of sediment DSi regeneration compared to the Siberian shelves. Link et al. (2013) also suggest that the high rates of DSi regeneration measured on the Mackenzie Shelf were driven by sampling conducted following a year of high diatom productivity and loading on the benthos due to proximity to the Cape Bathurst polynya, which exhibits high BSi export. Primary production on the Mackenzie Shelf is similar to other Arctic shelf areas but the Cape Bathurst polynya is characterized by a high proportion of diatoms and this area has previously been described as a "unique zone in biogenic silicate export from the euphotic zone" (Link et al., 2013; Sampei et al., 2011). These potential explanations are not mutually exclusive.

4.4. The Role of Shelf Sediments in the Arctic Ocean Si Cycle

While certainly not negligible as suggested by past studies, the inclusion of Si burial on continental shelves in the Arctic Ocean leads to only a modest 4.5% increase in Si outputs and does not imbalance the current system budget (Table 1). Unlike Si burial, Arctic Ocean continental shelves play a key role in Si recycling, and we estimate that Arctic Ocean shelves regenerate 680 ± 510 Gmol Si yr^{-1}—more than the amount of Si loaded by rivers and coastal erosion (370–590 Gmol Si yr^{-1}). Our sampling approach likely missed hotspots and hot moments of Si regeneration—see Link et al. (2013) for example,—but is nearly twice the annual regeneration of 370 Gmol Si yr^{-1} estimated by März et al. (2015) from a single core collected in the Northwest Passage. Seasonal variations in temperature, salinity, and timing of Si loading to the benthos could be additional sources of uncertainty in the annual rates of shelf Si regeneration.

We can test whether our estimates of sediment DSi regeneration and ASi burial are reasonable by considering the rate of BSi deposition and assuming that the fate of any BSi buried is either permanent burial or regeneration as DSi. Heiskanen and Keck (1996) report a mean sinking rate of BSi particulates >10 μm of 0.71 m d^{-1} and a water column BSi concentration of 0.3–4.1 μM in the Laptev Sea. Assuming uniform sinking through the water column, we can thus estimate a sediment loading rate of 212–291 μmol BSi m^{-2} d^{-1} by multiplying the BSi concentration and sinking rate. This rate is similar in range to our Si accumulation estimate of 385 μmol ASi m^{-2} d^{-1} (which also includes loading of riverine and coastal erosion particulates) and falls within the sediment Si accumulation range estimated by Ward et al. (2022b) of 130–5,310 μmol Si m^{-2} d^{-1} in the Barents Sea. Of this accumulation, we estimated a mean recycling flux of 295.1 μmol DSi m^{-2} d^{-1} and a mean burial of 44 μmol ASi m^{-2} d^{-1}. The sum of the burial and regeneration terms is within 15% of our mean daily loading estimate, and our burial rate

estimates are similar to estimates from the Barents Sea (21–27 μmol BSi m^{-2} d^{-1}; Ward et al., 2022b), indicating our approach is reasonable and that it is likely that burial efficiency in the Arctic Ocean is similar to the global burial efficiency.

5. Conclusions and Outlook

The Arctic Ocean is only 4.3% of the area and 1.4% of the volume of the global ocean (Jakobsson, 2002). Our estimate of Si burial on Arctic continental shelves indicates that they play a small role in the global marine Si cycle. The most recent estimate of the global marine Si sink is 9.2 ± 1.6 Tmol Si yr^{-1} (Tréguer et al., 2021). Our estimate of Si burial in the Arctic continental Ocean (70 Gmol Si yr^{-1}) is a small fraction of this, equal to less than 1% of the global marine Si sink. At the global scale, Si burial on Arctic continental shelves is small, but in the Arctic Ocean up to 4.5% of the Si loaded onto the system may be buried in shelf sediments. Conversely, our estimates of Si recycling to the water column on shelf sediments demonstrate they may be of similar importance to rivers in maintaining the availability of DSi in the water column and export of Si to other basins.

We estimate that Si burial (70 Gmol Si yr^{-1}) proceeds at approximately 10% of the rate of sediment DSi regeneration (680 Gmol Si yr^{-1}) on continental shelves in the Arctic Ocean. This value is quite similar to the estimated preservation ratio of BSi loaded on marine sediments globally (~11%, estimated by dividing mean BSi burial by mean BSi rain; Tréguer et al., 2021). As the Arctic Ocean warms in response to climate change, this ratio has either already begun to change or is likely to—Si dissolution kinetics are tightly linked with temperature and bacterial activity (Bidle et al., 2002; Kamatani, 1982), suggesting sediment DSi regeneration might increase, and burial may decrease as temperatures rise. Continued, or enhanced Si loading from Yedoma deposit erosion may further enhance the potential for Si burial and recycling in the Arctic Ocean. Changing riverine inputs, considering total discharge, total Si load, and the balance of DSi and ASi (Carey et al., 2020; Frey et al., 2007; Jankowski et al., 2023; Tank et al., 2023) will likely play an important role in regulating future rates of Si burial and recycling on Arctic continental shelves. Beyond the Arctic Ocean, exported Si from the Arctic Ocean fuels one of the most productive regions in the world, the North Atlantic. Greater future Si export to other ocean basins may have important implications for productivity, the magnitude of the marine biological pump, and removal of CO_2 from the atmosphere, underscoring the importance of understanding how Si cycling processes in the Arctic Ocean will respond to global change.

Data Availability Statement

All data reported in this study not found in the supplement are freely accessible from the Bolin Centre Database hosted by the Bolin Centre for Climate Research at Stockholm University (Ray et al., 2023; https://doi.org/10.17043/ray-2023-sediment-silicon-1).

Acknowledgments
We thank the crew and scientific team of the ISSS-2020 expedition. This work was funded by the Swedish Research Council VR (Grants 2018-05489 to B.W., 2021–06670 to J. M., as well as 2017-01601), the Swedish Research Council for Sustainable Development Formas (Grant 2018-01547 to B.W.), and Research Council of Norway (Grant 315317 for E.Y). JS and LS as well as the terrestrial Yedoma sampling were part of the joint National Environmental Research Council (UK) - Federal Ministry of Education and Research (BMBF; Germany) project #03F0806A, European Research Council starting grant #338335, German Research Foundation project POLYGON (He3622/16-1), and BMBF projects #3F0764B, # 03 G0836, and # 03G0569. We thank Daniel Conley for providing the external Si reference material.

References

Alfredsson, H., Clymans, W., Hugelius, G., Kuhry, P., & Conley, D. J. (2016). Estimated storage of amorphous silica in soils of the circum-Arctic tundra region. *Global Biogeochemical Cycles*, *30*(3), 479–500. https://doi.org/10.1111/1462-2920.13280

Alfredsson, H., Hugelius, G., Clymans, W., Stadmark, J., Kuhry, P., & Conley, D. J. (2015). Amorphous silica pools in permafrost soils of the Central Canadian Arctic and the potential impact of climate change. *Biogeochemistry*, *124*(1–3), 441–459. https://doi.org/10.1007/s10533-015-0108-1

Anderson, L. G., Björk, G., Jutterström, S., Pipko, I., Shakhova, N., Semiletov, I., & Wåhlström, I. (2011). East Siberian Sea, an Arctic region of very high biogeochemical activity. *Biogeosciences*, *8*(6), 1745–1754. https://doi.org/10.5194/bg-8-1745-2011

Anderson, L. G., Dyrssen, D. W., Jones, E. P., & Lowings, M. G. (1983). Inputs and outputs of salt, fresh water, alkalinity, and silica in the Arctic Ocean. *Deep-Sea Research, Part A: Oceanographic Research Papers*, *30*(1), 87–94. https://doi.org/10.1016/0198-0149(83)90036-5

Bidle, K. D., Manganelli, M., & Azam, F. (2002). Regulation of oceanic silicon and carbon preservation by temperature control on bacteria. *Science*, *298*(5600), 1980–1984. https://doi.org/10.1126/science.1076076

Bröder, L., Andersson, A., Tesi, T., Semiletov, I., & Gustafsson, Ö. (2019). Quantifying degradative loss of terrigenous organic carbon in surface sediments across the Laptev and East Siberian Sea. *Global Biogeochemical Cycles*, *33*(1), 85–99. https://doi.org/10.1029/2018gb005967

Bröder, L., Tesi, T., Andersson, A., Semiletov, I., & Gustafsson, Ö. (2018). Bounding cross-shelf transport time and degradation in Siberian-Arctic land-ocean carbon transfer. *Nature Communications*, *9*(1), 806. https://doi.org/10.1038/s41467-018-03192-1

Bröder, L., Tesi, T., Salvadó, J. A., Semiletov, I. P., Dudarev, O. V., & Gustafsson, Ö. (2016). Fate of terrigenous organic matter across the Laptev Sea from the mouth of the Lena River to the deep sea of the Arctic interior. *Biogeosciences*, *13*(17), 5003–5019. https://doi.org/10.5194/bg-13-5003-2016

Carey, J. C., Gewirtzman, J., Johnston, S. E., Kurtz, A., Tang, J., Vieillard, A. M., & Spencer, R. G. M. (2020). Arctic river dissolved and biogenic silicon exports—Current conditions and future changes with warming. *Global Biogeochemical Cycles*, *34*(3), e2019GB006308. https://doi.org/10.1029/2019GB006308

Codispoti, L. A., & Lowman, D. (1973). A reactive silicate budget for the Arctic Ocean. *Limnology & Oceanography*, *18*(3), 448–456. https://doi.org/10.4319/lo.1973.18.3.0448

Conley, D. J. (1998). An interlaboratory comparison for the measurement of biogenic silica in sediments. *Marine Chemistry*, *63*(1–2), 39–48. https://doi.org/10.1016/s0304-4203(98)00049-8

Conley, D. J., & Schelske, C. L. (2001). Biogenic silica. In J. P. Smol, H. J. Birks, & W. M. Last (Eds.), *Tracking environmental change using lake sediments: Biological methods and indicators* (pp. 281–293). Kluwer Academic Press.

DeMaster, D. J., Knapp, G. B., & Nittrouer, C. A. (1983). Biological uptake and accumulation of silica on the Amazon continental shelf. *Geochimica et Cosmochimica Acta*, *47*(10), 1713–1723. https://doi.org/10.1016/0016-7037(83)90021-2

DeMaster, D. J. (1981). The supply and accumulation of silica in the marine environment. *Geochemica et Cosmochimica Acta*, *45*(10), 1715–1732. https://doi.org/10.1016/0016-7037(81)90006-5

DeMaster, D. J. (2002). The accumulation and cycling of biogenic silica in the Southern Ocean: Revisiting the marine silica budget. *Deep Sea Research Part II: Topical Studies in Oceanography*, *49*(16), 3155–3167. https://doi.org/10.1016/s0967-0645(02)00076-0

DeMaster, D. J., Ragueneau, O., & Nittrouer, C. A. (1996). Preservation efficiencies and accumulation rates for biogenic silica and organic C, N, and P in high-latitude sediments: The Ross Sea. *Journal of Geophysical Research*, *101*(C8), 18501–18518. https://doi.org/10.1029/96jc01634

Dürr, H. H., Meybeck, M., Hartmann, J., Laruelle, G. G., & Roubeix, V. (2011). Global spatial distribution of natural riverine silica inputs to the coastal zone. *Biogeosciences*, *8*(3), 597–620. https://doi.org/10.5194/bg-8-597-2011

Frey, K. E., Siegel, D. I., & Smith, L. C. (2007). Geochemistry of west Siberian streams and their potential response to permafrost degradation. *Water Resources Research*, *43*(3), W03406. https://doi.org/10.1029/2006WR004902

Fuchs, M., Nitze, I., Strauss, J., Günther, F., Wetterich, S., Kizyakov, A., et al. (2020). Rapid fluvio-thermal erosion of a Yedoma permafrost cliff in the Lena River delta. *Frontiers in Earth Science*, *8*, 336. https://doi.org/10.3389/feart.2020.00336

Glud, R. N., Berg, P., Fossing, H., & Jørgensen, B. B. (2007). Effect of the diffusive boundary layer on benthic mineralization and O_2 distribution: A theoretical model analysis. *Limnology & Oceanography*, *52*(2), 547–557. https://doi.org/10.4319/lo.2007.52.2.0547

Gordeev, V. V., Martin, J. M., Sidorov, I. S., & Sidorova, M. V. (1996). A reassessment of the Eurasian river input of water, sediment, major elements, and nutrients to the Arctic Ocean. *American Journal of Science*, *296*(6), 664–691. https://doi.org/10.2475/ajs.296.6.664

Günther, F., Overduin, P. P., Sandakov, A. V., Grosse, G., & Grigoriev, M. N. (2013). Short- and long-term thermo-erosion of ice-rich permafrost coasts in the Laptev Sea region. *Biogeosciences*, *10*(6), 4297–4318. https://doi.org/10.5194/bg-10-4297-2013

Gustafsson, Ö., Van Dongen, B. E., Vonk, J. E., Dudarev, O. V., & Semiletov, I. P. (2011). Widespread release of old carbon across the Siberian Arctic echoed by its large rivers. *Biogeosciences*, *8*(6), 1737–1743. https://doi.org/10.5194/bg-8-1737-2011

Hawkings, J. R., Wadham, J. L., Benning, L. G., Hendry, K. R., Tranter, M., Tedstone, A., et al. (2017). Ice sheets as a missing source of silica to the polar oceans. *Nature Communications*, *8*(1), 14198. https://doi.org/10.1038/ncomms14198

Heiskanen, A. S., & Keck, A. (1996). Distribution and sinking rates of phytoplankton, detritus, and particulate biogenic silica in the Laptev Sea and Lena River (Arctic Siberia). *Marine Chemistry*, *53*(3–4), 229–245. https://doi.org/10.1016/0304-4203(95)00091-7

Hoffmann, S. S., Mcmanus, J. F., Curry, W. B., & Brown-leger, L. S. (2013). Persistent export of 231Pa from the deep central Arctic Ocean over the past 35,000 years. *Nature*, *497*(7451), 3–7. https://doi.org/10.1038/nature12145

Holmes, R. M., McClelland, J. W., Peterson, B. J., Tank, S. E., Bulygina, E., Eglinton, T. I., et al. (2012). Seasonal and annual fluxes of nutrients and organic matter from large rivers to the Arctic Ocean and surrounding seas. *Estuaries and Coasts*, *35*(2), 369–382. https://doi.org/10.1007/s12237-011-9386-6

Hydes, D., Aoyama, M., Aminot, A., Bakker, K., Becker, S., Coverly, S., et al. (2010). Determination of dissolved nutrients (N, P, Si) in seawater with high precision and inter-comparability using gas-segmented continuous flow analysers. In *The GO-SHIP repeat hydrography manual IOCCP report* (Vol. 134). Retrieved from http://archimer.ifremer.fr/doc/00020/13141/

Jakobsson, M. (2002). Hypsometry and volume of the Arctic Ocean and its constituent seas. *Geochemistry, Geophysics, Geosystems*, *3*(5), 1–18. https://doi.org/10.1029/2001gc000302

Jakobsson, M., Mayer, L. A., Bringensparr, C., Castro, C. F., Mohammad, R., Johnson, P., et al. (2020). The international bathymetric chart of the Arctic Ocean version 4.0. *Scientific Data*, *7*(1), 1–14. https://doi.org/10.1038/s41597-020-0520-9

Jankowski, K. J., Johnson, K., Sethna, L., Julian, P., Wymore, A. S., Shogren, A. J., et al. (2023). Long-term changes in concentration and yield of riverine dissolved silicon from the poles to the tropics. *Global Biogeochemical Cycles*, *37*(9), e2022GB007678. https://doi.org/10.1029/2022gb007678

Jones, E. P., & Coote, A. R. (1980). Nutrient distributions in the Canadian Archipelago: Indicators of summer water mass and flow characteristics. *Canadian Journal of Fisheries and Aquatic Sciences*, *37*(4), 589–599. https://doi.org/10.1139/f80-075

Kamatani, A. (1982). Dissolution rates of silica from diatoms decomposing at various temperatures. *Marine Biology*, *68*(1), 91–96. https://doi.org/10.1007/BF00393146

Kanevskiy, M., Shur, Y., Strauss, J., Jorgenson, T., Fortier, D., Stephani, E., & Vasiliev, A. (2016). Patterns and rates of riverbank erosion involving ice-rich permafrost (Yedoma) in northern Alaska. *Geomorphology*, *253*, 370–384. https://doi.org/10.1016/j.geomorph.2015.10.023

Karlsson, E., Gelting, J., Tesi, T., van Dongen, B., Andersson, A., Semiletov, I., et al. (2016). Different sources and degradation state of dissolved, particulate, and sedimentary organic matter along the Eurasian Arctic coastal margin. *Global Biogeochemical Cycles*, *30*(6), 898–919. https://doi.org/10.1002/2015GB005307

Lantuit, H., Overduin, P. P., Couture, N., Wetterich, S., Aré, F., Atkinson, D., et al. (2012). The Arctic coastal dynamics database: A New classification scheme and statistics on Arctic permafrost coastlines. *Estuaries and Coasts*, *35*(2), 383–400. https://doi.org/10.1007/s12237-010-9362-6

Lewis, K. L., van Dijken, G., & Arrigo, K. R. (2020). Changes in phytoplankton concentration now drive increased Arctic Ocean primary production. *Science*, *369*(6500), 198–202. https://doi.org/10.1126/science.aay8380

Link, H., Chaillou, G., Forest, A., Piepenburg, D., & Archambault, P. (2013). Multivariate benthic ecosystem functioning in the Arctic-benthic fluxes explained by environmental parameters in the southeastern Beaufort Sea. *Biogeosciences*, *10*(9), 5911–5929. https://doi.org/10.5194/bg-10-5911-2013

Martens, J., Romankevich, E., Semiletov, I., Wild, B., van Dongen, B., Vonk, J., et al. (2021). CASCADE – The Circum-Arctic Sediment CArbon DatabasE. *Earth System Science Data*, *13*(6), 2561–2572. https://doi.org/10.5194/essd-13-2561-2021

Martens, J., Wild, B., Semiletov, I., Dudarev, O. V., & Gustafsson, Ö. (2022). Circum-Arctic release of terrestrial carbon varies between regions and sources. *Nature Communications*, *13*(1), 5858. https://doi.org/10.1038/s41467-022-33541-0

März, C., Meinhardt, A. K., Schnetger, B., & Brumsack, H. J. (2015). Silica diagenesis and benthic fluxes in the Arctic Ocean. *Marine Chemistry*, *171*, 1–9. https://doi.org/10.1016/j.marchem.2015.02.003

Matsubara, F., Wild, B., Martens, J., Andersson, A., Wennström, R., Bröder, L., et al. (2022). Molecular-multiproxy assessment of land-derived organic matter degradation over extensive scales of the East Siberian Arctic Shelf Seas. *Global Biogeochemical Cycles*, *36*(12), e2022GB007428. https://doi.org/10.1029/2022gb007428

McClelland, J. W., Holmes, R. M., Peterson, B. J., Raymond, P. A., Striegl, R. G., Zhulidov, A. V., et al. (2016). Particulate organic carbon and nitrogen export from major Arctic rivers. *Global Biogeochemical Cycles*, *30*(5), 629–643. https://doi.org/10.1002/2015GB005351

Meire, L., Meire, P., Struyf, E., Krawczyk, D. W., Arendt, K. E., Yde, J. C., et al. (2016). High export of dissolved silica from the Greenland Ice Sheet. *Geophysical Research Letters*, *43*(17), 9173–9182. https://doi.org/10.1002/2016GL070191

Meredith, M., Sommerkorn, M., Cassotta, S., Derksen, C., Ekaykin, A., Hollowed, A., et al. (2019). Polar regions. In H. Pörtner, D. Roberts, V. Masson-Delmotte, P. Zhai, M. Tignor, E. Poloczanska, et al. (Eds.), *IPCC special report on the ocean and cryosphere in a changing climate*. https://doi.org/10.1016/S1366-7017(01)00066-6

Monhonval, A., Mauclet, E., Pereira, B., Vandeuren, A., Strauss, J., Grosse, G., et al. (2021). Mineral element stocks in the Yedoma Domain: A novel method applied to ice-rich permafrost regions. *Frontiers in Earth Science*, *9*, 703304. https://doi.org/10.3389/feart.2021.703304

Ng, H. C., Cassarino, L., Pickering, R. A., Woodward, E. M. S., Hammond, S. J., & Hendry, K. R. (2020). Sediment efflux of silicon on the Greenland margin and implications for the marine silicon cycle. *Earth and Planetary Science Letters*, *529*, 115877. https://doi.org/10.1016/j.epsl.2019.115877

Nishino, S., Shimada, K., Itoh, M., & Chiba, S. (2009). Vertical double silicate maxima in the sea-ice reduction region of the western Arctic Ocean: Implications for an enhanced biological pump due to sea-ice reduction. *Journal of Oceanography*, *65*(6), 871–883. https://doi.org/10.1007/s10872-009-0072-2

Nürnberg, D. (1996). Biogenic barium and opal in the shallow Eurasian Shelf sediments in relation to the pelagic Arctic Ocean environment. In R. Stein, G. Ivanov, M. Levitan, & K. Fahl (Eds.), *Surface-sediment composition and sedimentary processes in the Arctic Ocean and along the Eurasian Continental Margin* (pp. 96–118).

Obu, J., Westermann, S., Bartsch, A., Berdnikov, N., Christiansen, H. H., Dashtseren, A., et al. (2019). Northern Hemisphere permafrost map based on TTOP modelling for 2000–2016 at 1 km^2 scale. *Earth-Science Reviews*, *193*, 299–316. https://doi.org/10.1016/j.earscirev.2019.04.023

Osadchiev, A., Silvestrova, K., & Myslenkov, S. (2020). Wind-driven coastal upwelling near large river deltas in the Laptev and east-Siberian seas. *Remote Sensing*, *12*(5), 1–25. https://doi.org/10.3390/rs12050844

Pogojeva, M., Yakushev, E., Ilinskaya, A., Polukhin, A., Braaten, H. F., & Kristiansen, T. (2018). Experimental study of the influence of thawing permafrost on the chemical properties of sea water. *Russian Journal of Earth Sciences*, *18*(5), ES5002–6. https://doi.org/10.2205/2018ES000629

Prairie, Y. T. (1996). Evaluating the predictive power of regression models. *Canadian Journal of Fisheries and Aquatic Sciences*, *53*(3), 490–492. https://doi.org/10.1139/f95-204

Ragueneau, O., Schultes, S., Bidle, K., Claquin, P., & Moriceau, B. (2006). Si and C interactions in the world ocean: Importance of ecological processes and implications for the role of diatoms in the biological pump. *Global Biogeochemical Cycles*, *20*(4), 1–15. https://doi.org/10.1029/2006GB002688

Ray, N., Martens, J., Ajmar, M., Tesi, T., Yakushev, E., Gangnus, I., et al. (2023). The role of coastal Yedoma deposits and continental shelf sediments in the Arctic Ocean silicon cycle. https://doi.org/10.17043/ray-2023-sediment-silicon-1

R Core Team. (2014). R: A language and environment for statistical computing. Retrieved from http://www.r-project.org/

Sampei, M., Sasaki, H., Makabe, R., Forest, A., Hattori, H., Tremblay, J. É., et al. (2011). Production and retention of biogenic matter in the southeast Beaufort Sea during 2003–2004: Insights from annual vertical particle fluxes of organic carbon and biogenic silica. *Polar Biology*, *34*(4), 501–511. https://doi.org/10.1007/s00300-010-0904-y

Schirrmeister, L., Grosse, G., Wetterich, S., Overduin, P. P., Strauss, J., Schuur, E. A. G., & Hubberten, H. W. (2011). Fossil organic matter characteristics in permafrost deposits of the northeast Siberian Arctic. *Journal of Geophysical Research*, *116*(3), G00M02. https://doi.org/10.1029/2011JG001647

Schirrmeister, L., Kunitsky, V., Grosse, G., Wetterich, S., Meyer, H., Schwamborn, G., et al. (2011). Sedimentary characteristics and origin of the Late Pleistocene Ice Complex on north-east Siberian Arctic coastal lowlands and islands – A review. *Quaternary International*, *241*(1–2), 3–25. https://doi.org/10.1016/j.quaint.2010.04.004

Schirrmeister, L., Schwamborn, G., Overduin, P. P., Strauss, J., Fuchs, M. C., Grigoriev, M., et al. (2017). Yedoma Ice Complex of the Buor Khaya Peninsula (southern Laptev Sea). *Biogeosciences*, *14*(5), 1261–1283. https://doi.org/10.5194/bg-14-1261-2017

Stimmler, P., Goeckede, M., Elberling, B., Natali, S., Kuhry, P., Perron, N., et al. (2023). Pan-Arctic soil element bioavailability estimations. *Earth System Science Data*, *15*(3), 1059–1075. https://doi.org/10.5194/essd-15-1059-2023

Strauss, J., Laboor, S., Schirrmeister, L., Fedorov, A. N., Fortier, D., Froese, D., et al. (2021). Circum-Arctic map of the Yedoma permafrost domain. *Frontiers in Earth Science*, *9*, 758360. https://doi.org/10.3389/feart.2021.758360

Strauss, J., Schirrmeister, L., Mangelsdorf, K., Eichhorn, L., Wetterich, S., & Herzschuh, U. (2015). Organic-matter quality of deep permafrost carbon – A study from Arctic Siberia. *Biogeosciences*, *12*(7), 2227–2245. https://doi.org/10.5194/bg-12-2227-2015

Strauss, J., Schirrmeister, L., Wetterich, S., Borchers, A., & Davydov, S. P. (2012). Grain-size properties and organic-carbon stock of Yedoma Ice Complex permafrost from the Kolyma lowland, northeastern Siberia. *Global Biogeochemical Cycles*, *26*(3), GB3003. https://doi.org/10.1029/2011GB004104

Strickland, J., & Parsons, T. (Eds.). (1968). *A practical handbook of seawater analysis*. Queen's Printer.

Sun, X., Humborg, C., Mörth, C., & Brüchert, V. (2021). The importance of benthic nutrient fluxes in supporting primary production in the Laptev and East Siberian Shelf Seas. *Global Biogeochemical Cycles*, *35*(7), e2020GB006849. https://doi.org/10.1029/2020gb006849

Tank, S. E., McClelland, J. W., Spencer, R. G., Shiklomanov, A. I., Suslova, A., Moatar, F., et al. (2023). Recent trends in the chemistry of major northern rivers signal widespread Arctic change. *Nature Geoscience*, *16*(9), 789–796. https://doi.org/10.1038/s41561-023-01247-7

Terhaar, J., Kwiatkowski, L., & Bopp, L. (2020). Emergent constraint on Arctic Ocean acidification in the twenty-first century. *Nature*, *582*(7812), 379–383. https://doi.org/10.1038/s41586-020-2360-3

Terhaar, J., Lauerwald, R., Regnier, P., Gruber, N., & Bopp, L. (2021). Around one third of current Arctic Ocean primary production sustained by rivers and coastal erosion. *Nature Communications*, *12*(1), 169. https://doi.org/10.1038/s41467-020-20470-z

Torres-Valdés, S., Tsubouchi, T., Bacon, S., Naveira-Garabato, A. C., Sanders, R., McLaughlin, F. A., et al. (2013). Export of nutrients from the Arctic Ocean. *Journal of Geophysical Research: Oceans*, *118*(4), 1625–1644. https://doi.org/10.1002/jgrc.20063

Tréguer, P., Bowler, C., Moriceau, B., Dutkiewicz, S., Gehlen, M., Aumont, O., et al. (2018). Influence of diatom diversity on the ocean biological carbon pump. *Nature Geoscience*, *11*(1), 27–37. https://doi.org/10.1038/s41561-017-0028-x

Tréguer, P. J., & Pondaven, P. (2000). Silica control of carbon dioxide. *Nature*, *406*(6794), 358–359. https://doi.org/10.1111/j.1463-1326.2010.01202.x

Tréguer, P. J., Sutton, J. N., Brzezinski, M., Charette, M. A., Devries, T., Dutkiewicz, S., et al. (2021). Reviews and syntheses: The biogeochemical cycle of silicon in the modern ocean. *Biogeosciences*, *18*(4), 1269–1289. https://doi.org/10.5194/bg-18-1269-2021

Tremblay, J. É., Raimbault, P., Garcia, N., Lansard, B., Babin, M., & Gagnon, J. (2014). Impact of river discharge, upwelling and vertical mixing on the nutrient loading and productivity of the Canadian Beaufort Shelf. *Biogeosciences*, *11*(17), 4853–4868. https://doi.org/10.5194/bg-11-4853-2014

Turner, R. E., & Rabalais, N. N. (1994). Coastal eutrophication near the Mississippi river delta. *Nature*, *368*(6472), 619–621. https://doi.org/10.1038/368619a0

Van Cappellen, P., & Qiu, L. (1997). Biogenic silica dissolution in sediments of the Southern Ocean. II. Kinetics. *Deep-Sea Research Part II Topical Studies in Oceanography*, *44*(5), 1129–1149. https://doi.org/10.1016/s0967-0645(96)00112-9

Wang, K., Zhang, T., & Yang, D. (2021). Permafrost dynamics and their hydrologic impacts over the Russian Arctic drainage basin. *Advances in Climate Change Research*, *12*(4), 482–498. https://doi.org/10.1016/j.accre.2021.03.014

Ward, J. P., Hendry, K. R., Arndt, S., Faust, J. C., Freitas, F. S., Henley, S. F., et al. (2022a). Stable silicon isotopes uncover a mineralogical control on the benthic silicon cycle in the Arctic Barents Sea. *Geochimica et Cosmochimica Acta*, *329*, 206–230. https://doi.org/10.1016/j.gca.2022.05.005

Ward, J. P., Hendry, K. R., Arndt, S., Faust, J. C., Freitas, F. S., Henley, S. F., et al. (2022b). Benthic silicon cycling in the Arctic Barents Sea: A reaction–transport model study. *Biogeosciences*, *19*(14), 3445–3467. https://doi.org/10.5194/bg-19-3445-2022

Wegner, C., Bennett, K. E., de Vernal, A., Forwick, M., Fritz, M., Heikkilä, M., et al. (2015). Variability in transport of terrigenous material on the shelves and the deep Arctic Ocean during the Holocene. *Polar Research*, *34*(1), 24964. https://doi.org/10.3402/polar.v34.24964

Wild, B., Andersson, A., Bröder, L., Vonk, J., Hugelius, G., McClelland, J. W., et al. (2019). Rivers across the Siberian Arctic unearth the patterns of carbon release from thawing permafrost. *Proceedings of the National Academy of Sciences of the United States of America*, *116*(21), 10280–10285. https://doi.org/10.1073/pnas.1811797116

Wild, B., Ray, N. E., Lett, C., Davies, A. J., Kirillova, E., Holmstrand, H., et al. (2023). Nitrous oxide dynamics in the Siberian Arctic Ocean and vulnerability to climate change. *Journal of Geophysical Research: Biogeosciences*, *128*(5), e2022JG007326. https://doi.org/10.1029/2022jg007326